J Extra Corpor Technol. 2022;54:107–14
The Journal of ExtraCorporeal Technology

Original Articles

A New Evaluation *Q*-Factor to Be Calculated for Suction Geometries as a Basis for Smooth Suction in the Operating Field to Ensure the Highest Possible Blood Integrity for Retransfusion Systems

Ireneusz Iwanowski;*[a] Jan Böckhaus;†[a] Pascal Richardt;† Ingo Kutschka;* Gunnar G. Hanekop;‡[b] Martin G. Friedrich*[b]

**Department of Thoracic, Cardiac and Vascular Surgery, †Clinic for Nephrology and Rheumatology, and ‡Department of Anesthesiology, University Medical Center Göttingen, Göttingen, Germany*

Abstract: Blood hemolysis caused by mechanical impact is a serious problem in medicine. In addition to the heart-lung machine (artificial surfaces, flow irritating connection points) which contributes to hemolysis, blood suction and surgical suction devices are influencing factors. Goal of our research is to develop best flow optimizing suction geometry that represents the best compromise between all influencing effects. Based on data that negative pressure and turbulence have a negative impact on blood components, 27 surgical suction tips have been examined for acoustic stress and negative pressure behavior. Furthermore, a dimensionless factor *Q* was introduced to assess the overall performance of the suction tips investigated. **Keywords:** flow optimization, suction tip, suction systems, noise in OR, blood retransfusion, cell-saver, retransfusion systems, blood integrity. *J Extra Corpor Technol. 2022;54:107–14*

The aim of this work was to assess surgical suction tips (SST) (Fig. 1) in terms of mechanical stress on blood cells and associated hemolysis (1–5). Another problem is blood–air contact that cannot be avoided but can be reduced by optimizing the SST tip geometry. Empirical correlations are widely used for the estimation of flow-induced hemolysis in blood-contacting medical devices. Most of the studies use power law to correlate shear stress and exposure time; power law $= AT^{\alpha}t^{\beta}$ (6,7), A, α, and β are estimated as 3.6210^{-5}, 2.416, and .785 respectively (6), whereas in a recent study (7), $A = 1.228\ 10^{-5}$, $\alpha = 1.9918$, and $\beta = .6606$ are suggested. Zhang et al. (7) formula predicts .1% hemolysis for an exposure time of 887 ms under a shear rate of 30,000 seconds^{-1} while that of Giersiepen et al. (6) estimates 1% hemolysis under the same flow conditions. One order of magnitude difference between these in vitro models suggests that empirical estimations strongly depend on test device and experimental conditions. The occurrence of turbulence and the associated stress on blood cells during medical surgical suction can be correlated very well with the volume and frequency range generated by the suction process. Any flow interruptions can be assigned to an acoustic signal. For this purpose, the acoustic behavior was investigated. SSTs are used during nearly all operations to have a clear view on the operating field—but also to aspirate fluids, such as blood, to retransfuse it after processing. Maintaining as much as possible integrity of the aspirated blood is important for the subsequent preparation for retransfusion (e.g., cell-saver).

Friedrich et al. (8) have shown that an optimized suction head geometry significantly reduces turbulence and

Received for publication October 11, 2021; accepted April 5, 2022.
Address correspondence to: Ireneusz Iwanowski, PhD, University Medical Center Göttingen: Georg-August-Universitat Gottingen Universitatsmedizin, Robert-Koch-Str. 40, Goettingen, Lower Saxony 37075, Germany. E-mail: irek.iwanowski@med.uni-goettingen.de
[a]These authors contributed equally to this work.
[b]These authors contributed equally and share senior authorship.
The senior author has stated that the authors have reported no material, financial, or other relationship with any healthcare-related business or other entity whose products or services are discussed in this paper.

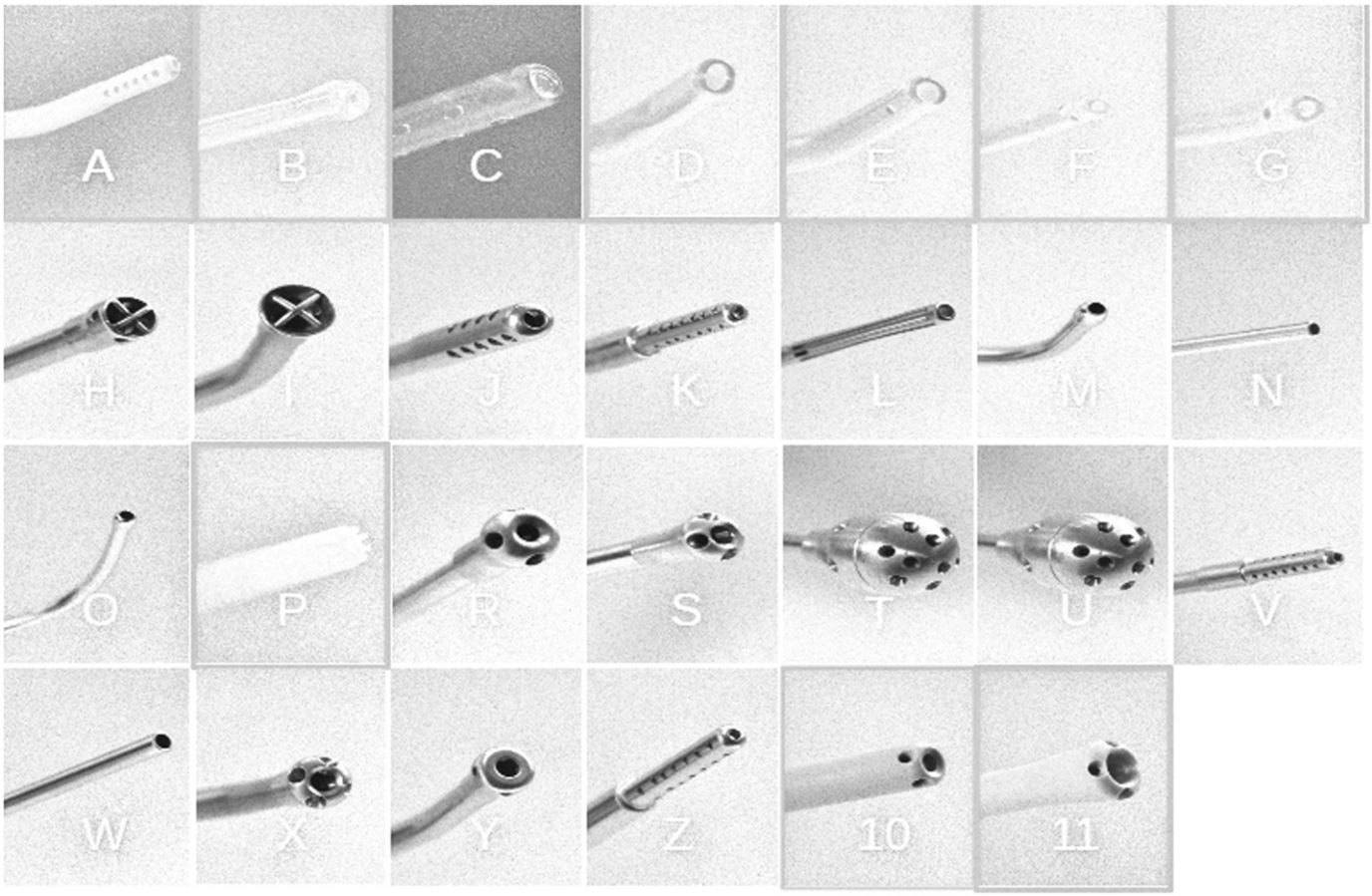

Figure 1. An overview of all SST examined. Letters represent commercial SSTs while numbers represent those developed in-house.

thus also noise development. On the one hand, this reduces noise pollution, especially in emergency situations, and on the other hand, it is associated with less stress for the blood cells. In vitro, Budde et al. (9) were able to show that there was significantly less hemolysis and significantly less misactivation of platelets (14) with preserved cross-linking ability. The topic is of increasing interest, as a significant decline in blood donation has been a problem and is currently aggravating. This shortage of allogeneic blood has become even more serious in the current pandemic situation (10). Thus, blood-saving including optimized suction procedures must contribute to making retransfusions of intraoperatively collected blood more probable and safe. The optimization tests on suction heads carried out by our research group at the University Medical Center Göttingen may help to reach this goal.

Another aim of this work is the introduction of a dimensionless number for SST performance, the so-called *Q*-factor. In this quantity, physical parameters such as pressure behavior, acoustic load, which correlates with generated turbulence, are to be mapped.

EXPERIMENT

Methods

Based on previous results (8,9), 25 standard SST models with different geometries were investigated in terms of their pressure-flow relationships. In a recirculation model (roller pump Polystan type Modular No. 1603, Vaerlose, Denmark) via tubes connected to a fluid sample tank (1/4″, 6.3 mm tube system, HMT-Medizintechnik GmbH, Maisach, Germany), measurements were performed in two different setups: 1) studies with completely diving SSTs and 2) studies with SSTs on surface. The flow-dependent (50 up to 1,950 mL/minute) noise emission (db[A] 10 cm), acoustic quality, Fast Fourier Transform (FFT), and changes of pressure were measured in the tube system (Figure 2). After an interim analysis, the learned relationships were translated into new suction head geometries in an iterative process. The best ones were identified and four new geometries were derived and drawn (Sharp3D V 4.6.0; Sharp3D Zrt., Budapest, Hungary).

Measurement tools: to verify the results, in addition to the registration of pressure-flow relationships (pressure

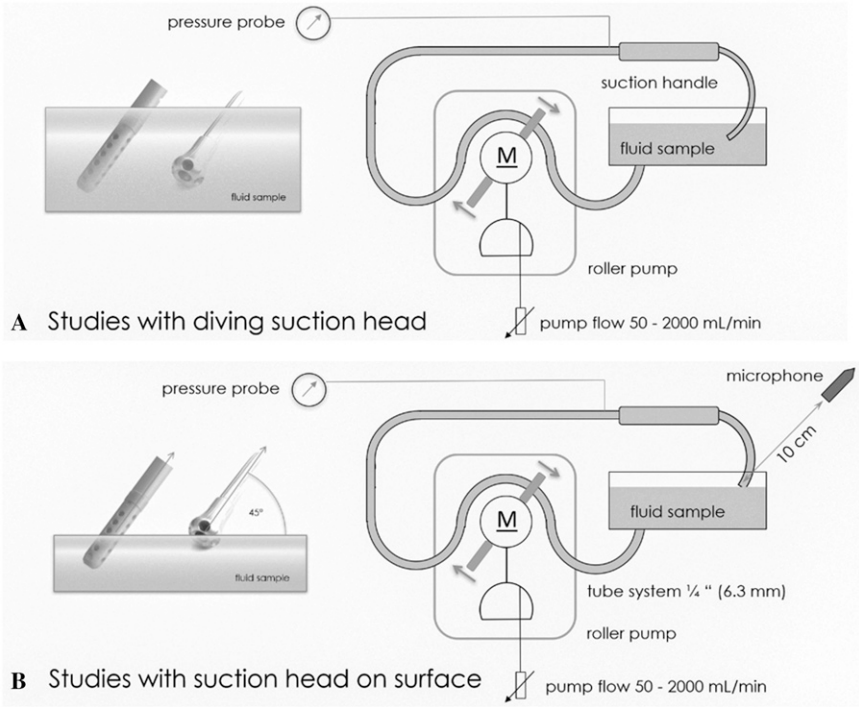

Figure 2. In vitro setup for investigations in two conditions. (A) SST model is diving (5 cm under surface). (B) SST model is fixed 45° to the fluid-air boundary. The half number of side holes are diving in the fluid, the others are in the air. Pressure measurements were taken near to the suction handheld, noise (sound pressure and frequency analysis) was taken in 10 cm distance to the suction head using an ultra linear measurement microphone.

measurement and recording, time window 1 ms, Harvard Aparatus, Hugo Sachs Elektronik, March-Hugstetten, Germany), high-resolution audio recording (uncompressed wave, 96 kHz, 24 bit, DR-100, TASCAM, TEAC Europe GmbH, Wiesbaden, Germany) was performed digitally using a unilinear measurement microphone (ECM-8000, BEHRINGER Spezielle Studiotechnik GmbH, Willich-Münchheide, Germany). In the same way as (9) noise levels were measured and recorded over 10-seconds intervals (dB[A], Voltcraft sound level recorder SL-451, 125 ms peaks, 31.5 Hz to 8 kHz, at distance 10 cm). The frequency spectra were graphically displayed as a noise map (Fast Fourier Analysis as spectroscopy and spectrography during 5 seconds, Hamming-filter, 20 Hz to 30 kHz, FFT Size 8192, Sequoia 14.1.0.157 DC2, 64 bit, Magix Software GmbH, Berlin, Germany). To bring physical measurements closer to the special flow properties of blood, after initial measurements with water, these additional investigations were performed with an artificial substitute fluid that mimics the viscosity of blood (8).

Statistic

Groups were compared by one-way ANOVA followed by Tukey's multiple comparisons tests and *p*-values of less than .05 were defined as statistically significant. Statistical calculations were performed with GraphPad PRISM7 (GraphPad Software Inc., La Jolla, CA).

RESULTS

Acoustical Behavior

Fitting model. This section deals with the noise generated by turbulent flow. For this, a different approach is required for evaluating the fluid in terms of pressure and even density. The original FIN theory and expressions are given by the aeroacoustic model of Ligthhill (11), using Einstein notation, as given below:

$$\frac{1}{c_0}\frac{\partial^2}{\partial t^2} - \nabla p^2 = \frac{\partial^2 T_{ij}}{\partial x_i \partial x_j} \text{ where } T_{ij} = \rho v_i v_j \quad (1)$$

Landau Lifshitz equation

Whenever the fluid can be compressed, pressure p variation is accompanied by density ρ variation, the expression of which is:

$$\frac{\partial^2 \rho}{\partial t^2} - c_0 \frac{\partial^2 \rho}{\partial x_i \partial_j} = \frac{\partial^2 v_i v_j}{\partial x_i \partial x_j} \quad (2)$$

Lighthill's equation

Thus, turbulence collaterally generates pressure and density variation in the fluid. The former cause the noise, and as such, are deemed to be sound sources (12).

In other words, as we want to reduce turbulence caused by the SSTs, their acoustic behavior is of great importance. Since only discrete values *db* (Figure 3) were recorded as a function of flow velocities, it was necessary

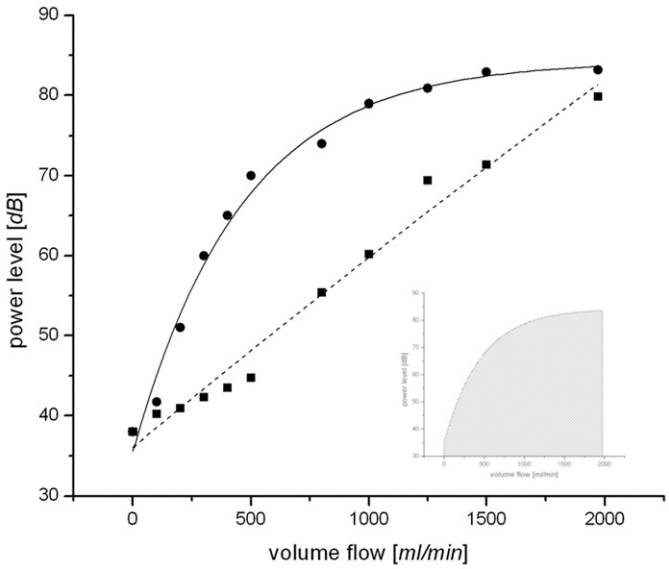

Figure 3. Example of two surgical suction tips *db*-Data: Tip ● [A-Model] and ■ Tip [11-Model], fitted by Eq. (4). Figure inside "filled area" represents area integral A_{db} calculations by Eq. (5).

to extrapolate the values. It is well known that the Reynolds number is an important parameter for identification of turbulence. Under simplified conditions (tube), the following equation applies to the Reynolds number, *Re*:

$$Re = \frac{vd\rho}{\eta} \text{ or } Re = \frac{vL}{\nu} \tag{3}$$

Reynolds number

where, v represents the average velocity, ρ liquid density, d pipe internal diameter, η absolute viscosity, L length, and V kinematic viscosity. Thus, number *Re* is a dimensionless value. If we leave density, diameter, and viscosity constant, it is obvious that *Re* is proportional to v. Under normal conditions (simple geometries), it is justified to assume a linear behavior for the values (*dB* or *p*) studied. Unfortunately, their behavior is a little bit more complicated. Geometries are very variable and parameters such as density ρ at the location of interest are not stable, they are rather nonlinear and chaotic in nature. Looking at Eqs. (1) and (2), and considering that the acoustic behavior is represented by logarithmic functions, it is obvious to use a nonlinear function for fitting the data, like exponential decay of first order:

$$L_{db}(Q) = Y_0 + A_0 exp(-Q/T_0) \tag{4}$$

Exponential decay of first order

where Q denotes dV/dt.

Acoustic load. One of the objectives of the present work is to make a qualitative assessment of different SSTs. An important characteristic for this is the acoustic load, which contributes to hemolysis. To convert this into a quantitative statement, the area integral under the fitted curves A_{db} for each suction head was calculated and compared with one another:

$$A_{db} = \int_{Q_{\min}}^{Q_{\max}} L_{dB}\, dQ \tag{5}$$

Area integral of acoustic load

A comparison of all suction heads examined shows a significant difference between the commercially available ones and the newly developed models. On average, the commercially available suction tips carried higher acoustic load (see Table 1). Significant differences can be observed especially in the normal working range between 750 and 1,500 mL/min. While the commercial SSTs range between 70 and 80 dB, the self-developed tips show a very slow increase and range between 45 and 65 dB.

Acoustic dynamic. An interesting question is posed by the dynamic progression of volume sound as a function of flow rate. For this purpose, an interpolated function is derived by:

$$D_{db} = \frac{dL_{db}}{dQ} \tag{6}$$

Derivative of volume sound

If we look at the two extreme representatives of "noisy" and "quiet" SSTs, (model-A and model-11)

Table 1. *Q*-factor overview.

Suction Tip	$\frac{A_{db}}{A_{max}}$	$\frac{A_{PPI}}{A_{Pmax}}$	$\frac{A_{PPS}}{A_{Pmax}}$	$\frac{A_{PSI}}{A_{Pmax}}$	$\frac{A_{PSS}}{A_{Pmax}}$	*Q*-Factor
11	.61	.12	.05	.08	.08	.94
10	.62	.13	.06	.08	.05	.94
8	.68	.12	.08	.08	.04	1.00
Y	.69	.15	.11	.09	.03	1.07
D	.65	.30	.07	.07	.05	1.10
P	.64	.22	.10	.10	.08	1.14
E	.66	.25	.09	.06	.08	1.14
C	.70	.29	.07	.06	.08	1.17
I	.68	.31	.09	.06	.06	1.20
J	.65	.32	.08	.07	.09	1.21
H	.73	.26	.07	.08	.07	1.21
W	.74	.22	.18	.12	.05	1.31
U	.61	.38	.13	.11	.09	1.32
Z	.70	.20	.17	.17	.08	1.32
B	.69	.36	.12	.11	.09	1.37
S	.69	.37	.14	.12	.09	1.41
L	.76	.31	.17	.12	.07	1.43
R	.69	.37	.12	.15	.13	1.46
T	.65	.41	.14	.09	.18	1.47
G	.70	.53	.17	.06	.08	1.54
F	.68	.62	.24	.04	.07	1.65
V	.75	.43	.24	.20	.05	1.67
A	.81	.52	.30	.20	.16	1.99
K	.78	.64	.24	.20	.14	2.00
M	.70	.51	.45	.38	.33	2.37
N	.85	.62	.52	.23	.20	2.42
O	.80	.72	.73	.34	.32	2.91

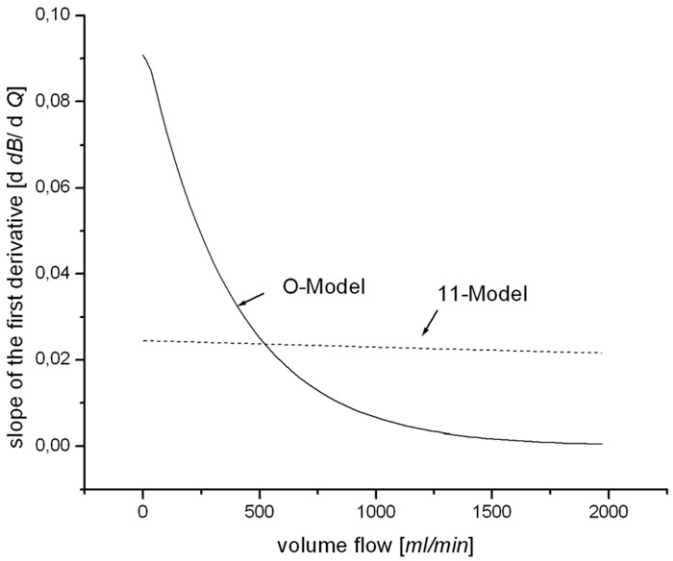

Figure 4. Example of two SST slope data of the first derivative: black curve, Tip [O-Model] and dashed curve, Tip [11-Model].

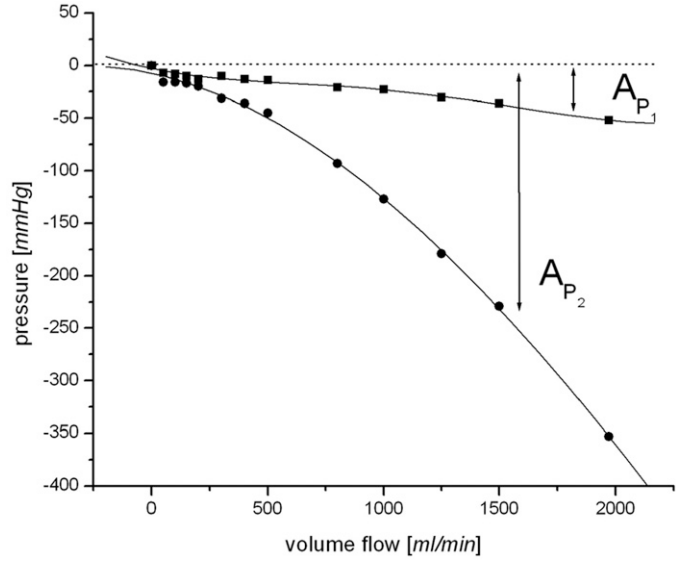

Figure 5. Example of two STT pressure data-sets: ● Tip [A-Model] and ■Tip [11-Model], fitted by a polynomial of forth degree. A_p represents the area between fitted curve and zero line (dotted).

(Fig. 4), significant differences in the dynamic development of volume sound can be seen.

Although the commercial model has a rapid entry into the higher flow rate range (see Figure 3), the optimized tip behaves very linearly. As mentioned before, especially in the interesting working range (750 and 1,500 mL/min), the volume values of the optimized SSTs are far below those of the commercially available ones. This leads us to hypothesize that the development of volume sound in dependence on the flow rate, is decisive for gentle suction. For this purpose, we define out a new qualification parameter. We distinguish between convex and concave behaviors of the acoustic dynamic:

$$\frac{d^2 L_{db}(Q)}{d^2 Q} > 0 \quad \text{concave behavior} \tag{7}$$

$$\frac{d^2 L_{db}}{d^2 Q} \lesssim 0 \quad \text{convex behavior} \tag{8}$$

Second derivation of volume sound

Pressure Behavior

A very important parameter in the consideration of the influence of the SST on blood integrity is pressure behavior. For this purpose, the SSTs were examined under various conditions. Pressure measurements have been performed as shown in Figure 2. As can be seen in Figure 5, in the case of the immersed model-A and model-11, the area between the X-axis and the interpolated data is decisive for the pressure behavior. The data points were fitted with a fourth-degree polynomial. The closer the curve is to the X-axis, the smaller the negative pressure acting on the blood components. We, therefore, investigated this behavior and included it into the definition of the Q-factor.

$$A_p = \left| \int P dQ \right| \tag{9}$$

Area integral

Performance at a glance. The aim of this work is to introduce a quality factor Q for comparison of damage potential of SSTs. For acoustic load, we have considered the area under the curve as decisive because it represents the total acoustic load of the SSTs. It is evident that the smaller the area especially in the normal work range, the lower the acoustic load, and therefore, the load on the blood components. We can write

$$A = \frac{A_{db}}{A_{max}} \tag{10}$$

Relation between max. acoustic load and acoustic load

where $A_{max} = \left(L_{db}^{max} - L_{db}^{min}\right)(Q_{max} - Q_{min})$. According to this, Eq. (10) ranges between 0 and 1, where 1 would be the most unfavorable (very loud) value and 0 the best, although this value will never be reached, as the area is always greater than 0. However, the smaller the ratio, the better the acoustic behavior. Next, we focused on the acoustic dynamics behavior. Therefore, we have considered the convexity and concavity in Eqs. (7) and (8) of the acoustic course and have looked at the second derivative of the interpolated functions. If the second derivative was greater than 0, i.e., the course was concave, then acoustic performance of the SSTs was worse;

if the second derivative was equal or less than 0, acoustic performance was better. Based on this empirical fact, we introduce the parameter D for which holds:

$$\text{If } D = \frac{d^2 L_{db}(Q)}{\mathrm{d}^2 Q} > 0 \text{ than}(1); \text{ if } D \lesssim 0 \text{ than } (-1)$$

Second derivation of acoustic load : Decision equation (11)

During our studies, we have measured the pressure behavior of the SSTs in the submerged state and in the boundary position between liquid and air at an angle of 45°. The pressure was recorded both at the suction tip and in the vicinity of the pump. As already mentioned, the pressure behavior is very crucial for the integrity of the blood components, and is therefore, an important parameter for the determination of the Q-factor. For this purpose, the area between the zero-axis and the close-fitting pressure curve was determined:

$$A_{px} = \mid \int P_x dQ \mid \quad (12)$$

Area integral of pressure

where x is a free variable for: p_{PI}, pressure Pump-Suction-Immersed, p_{PS}, pressure Pump-Suction-Surface, p_{SI} pressure Suction-Immersed and p_{SS}, and pressure Suction-Surface. This leads to:

$$P = \frac{A_{px}}{A_p^{max}} \quad (13)$$

Relation between max. pressure and pressure

The Q-factor we are proposing thus composed of (Fig. 7):

$$\mathrm{Q} = \mathrm{A} + \mathrm{D} + P_{PI,PS,SI,SS} \quad (14)$$

Q-factor equation

The maximum possible value for our Q-factor is 6. It should be mentioned this is purely an empirical relationship, an aid to verify the performance of individual SSTs in terms of their influence on blood integrity. In particular, the parameter D will have to be supplemented by a weighting factor in later studies. For this discussion, the parameter is set to 0 for all SSTs. Thus, all Q-factors for the SSTs measured, range between 0 and 5. The calculated values for the Q-factor are given in Table 1 illustrates in Figure 6.

DISCUSSION

The SSTs examined show very different behavior with regard to acoustic load and pressure behavior. It is not possible to make a general conclusion, that suction tips that are particularly loud and thus lead to increased flow interruptions, have negative pressure behavior. If we look at the commercial models (I, J, and H) (see Table 1), one can see that they exhibit gentle pressure behavior despite pronounced acoustic stress. However, there are also suction tips that exhibit both a strong acoustic load and a strong negative pressure load. These include the models (A, K, M, N, and O). Figure 9 illustrates the different contributions of the investigated variables to the total Q-factor. If one compares the Q-factors of model-11 ($Q = .94$) and model-O ($Q = 2.91$), a clear difference in physical behavior can be seen. Assuming that turbulence is accompanied by acoustical response and that negative pressure promotes the development of hemolysis, the conclusion can be drawn, that a small ρ-factor value

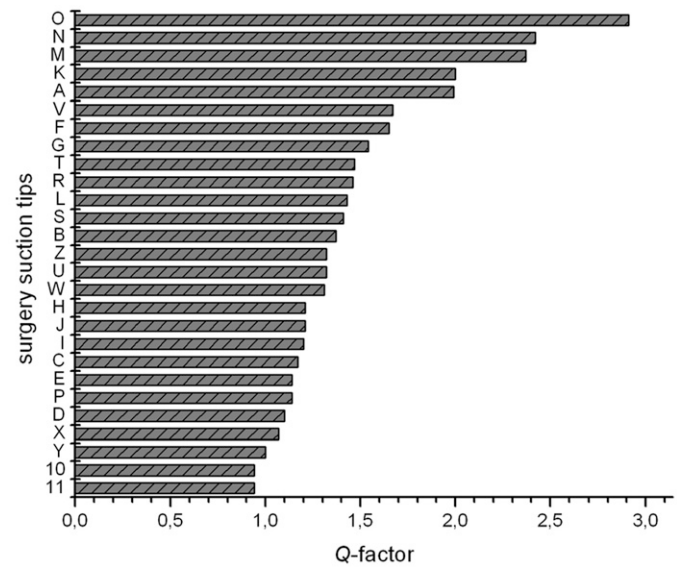

Figure 6. Q-factors of all investigated SSTs. Smaller value means better performance.

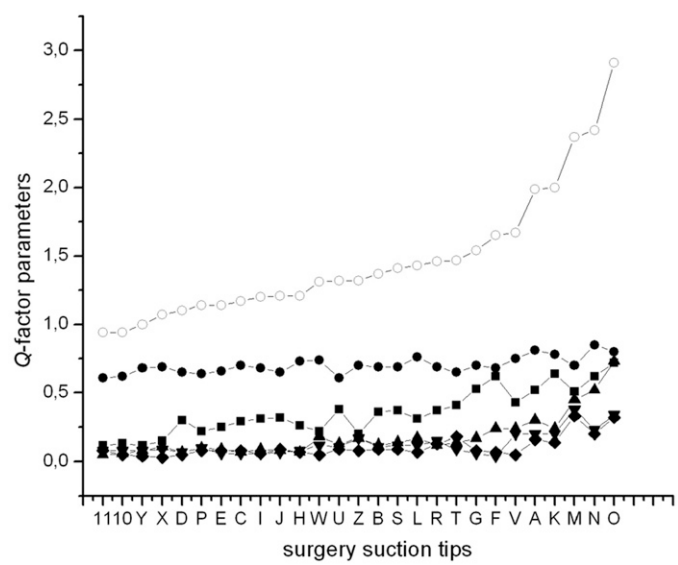

Figure 7. Q-factor components for: acoustic load ○-A, for pressure Pump-Suction-Immersed ■, pressure Pump-Suction-Surface ▲, pressure Suction-Immersed ▼, pressure Suction-Surface ◆.

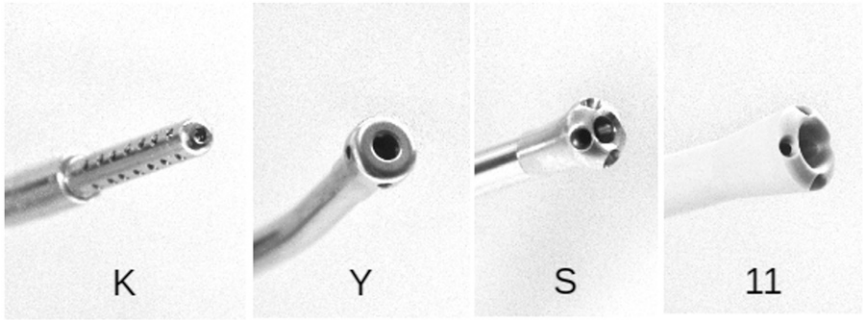

Figure 8. Example of different geometries of SSTs.

indicates gentle blood treatment. It also seems that the optimized models 10 and 11 fulfill this task well.

We look at the geometries of the SSTs studied (Figure 8) to better understand the impact on the *Q*-factor: a suction tip with a high *Q*-factor; model-K (2.00), a suction tip from the midfield Model-S (1.41), and two suction tips with a small *Q*-factor, the model-Y (1.00), and the optimized model-11 (.94). In Figures 9 and 10, we present fitted data of these models or the acoustic load and for the negative pressure behavior. It is obvious that suction cups with multiple side holes at the have worse *Q*-factors. In this context, we relate the geometry to the turbulent behavior. Suction tips with multiple side holes promote flow breaks and turbulent behavior. This can be explained by different velocity and pressure profiles near the inlet. In addition, there is a strong mixing with ambient air. This locally leads to strong density and viscosity variations, which favors turbulent behavior as well. Another interesting aspect of the different geometries is the inlet shape of the suction tip, no final assessment can be made at this point. However, it is conspicuous that suction tips with gentle inlet profiles obtain better *Q*-factors. This may be due to the fact that abrupt radial changes at the inlet promote turbulent behavior of fluids.

CONCLUSION

In this investigation, 27 different SST were studied. The focus primarily was on destructive acoustic behavior on blood components. Furthermore, different pressure measurement scenarios were also performed because higher negative pressures also may have a negative influence on blood integrity (13). Among the 27 SST, commercial ones as well as self-developed were investigated and successively optimized regarding their acoustic and pressure behaviors. Based on investigations and multiple shape adjustments, an optimized geometry was found for a suction tip that

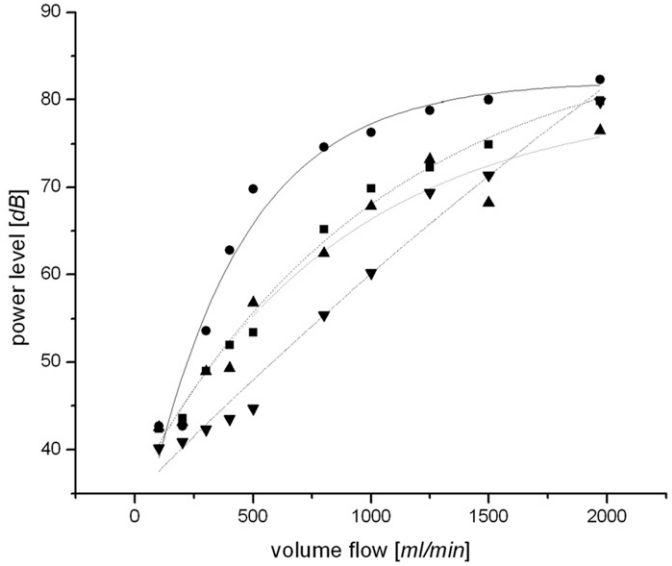

Figure 9. Comparison of *db*-data: ●-Model-K, -■Model-S, ▲-Model-Y, and ▼-Model-11. Data fitted by Eq. (4).

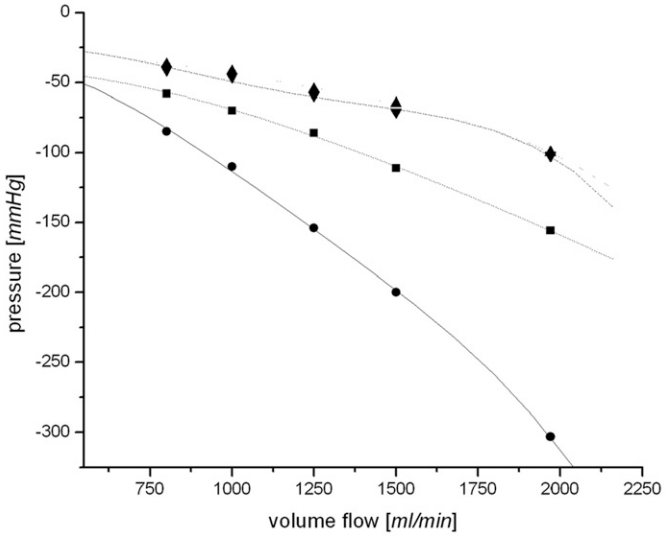

Figure 10. Comparison of db-data: ●-Model-K, -■Model-S, ▲-Model-Y, and ▼-Model-11. Data fitted by polynomial fourth degree.

exhibits particularly gentle suction behavior. To ensure an assessment of the performance of individual SST on blood integrity, an empirical quality factor Q was introduced. This takes into account both the acoustic and the pressure behaviors. But we have to emphasize that this is purely descriptive empirical formula that does not reflect a stringent physical relationship. Individual measurement behaviors are taken into account in the sum. It is also necessary to supplement this correlation with the weightings of individual components. However, this can only be done with explicit studies of hemolysis behavior. Under the premise that turbulence correlates with density variation and the fact that it has a negative influence on hemolysis, it is obvious that this approach is logic. Furthermore, it is important to include the pressure behavior to get a complete picture of the performance of individual SST. If the tips examined are considered in relation to the Q-factor, their discussed behavior is not only qualitatively, but also quantitatively represented in a ranking. Since the proposed Q-factor equally weights all determined quantities, it is of particular interest to determine the weighting factors experimentally, by hemolysis measurements. Such measurements would increase the significance of the Q-factor. Currently, our research group is conducting experiments with human blood. We hope to establish a direct connection between the Q-factor and the hemolysis level. Last but not least, our goal is to develop gentle suction cups to ensure both suction performance and blood recovery.

ACKNOWLEDGMENTS

We thank the programmers of Sharp3D Zrt., Hungary, Budapest, Bajcsy-Zylinskzky ut 12 for providing us with a highly functional CAD 3D software free of charge.

REFERENCES

1. Herbertson L, Olia S, Daly A, et al. Multilaboratory study of flow-induced hemolysis using the FDA benchmark nozzle model. Artif Organs. 2014;39:237–48.
2. Deplano V, Knapp Y, Bailly L, et al. Flow of a blood analogue fluid in a compliant abdominal aortic aneurysm model: Experimental modeling. J Biomech. 2014;47:1262–9.
3. Fardin K, Peshala PT, Hansen AM. Prediction of turbulent shear stresses through dysfunctional bileaflet mechanical heart valves using computational fluid dynamics. In: 3rd Thermal and Fluids Engineering Conference (TFEC); 2018. TFEC-2018-22070.
4. Abbasi M, Alexander F, Hamid EZ, et al. Erythrocyte-erythrocyte aggregation dynamics under shear flow. Phys Rev Fluids. 2018;6: 023602.
5. Sohrabi S, Yaling L. A cellular model of shear-induced hemolysis. Artif Organs. 2017;41:E80–91.
6. Giersiepen M, Wurzinger LJ, Opitz R, et al. Estimation of shear stress-related blood damage in heart valve prostheses. Artif Organs. 1990;13:300–9.
7. Zhang T, Taskin ME, Fang HB, et al. Study of flow induced hemolysis using novel coquette type blood shearing devices. Artif Organs. 2011;35:1180–6.
8. Friedrich MG, Tirilomis T, Kollmeier JM, et al. Modifications of surgical suction tip geometry for flow optimisation: Influence on suction-induced noise pollution. Surg Res Pract. 2018;2018:3074819.
9. Budde H, Riggert J, Vormfelde S, et al. The effect of a novel turbulence-controlled suction system in the prevention of hemolysis and platelet dysfunction in autologous surgery blood. Perfusion. 2019;34:58–66.
10. Chandler T, Neuman-Böhme S, Sabat I, et al. Blood donation in times of crisis: Early insight into impact of COVID-19 on blood donors and their motivation to donate across European countries. Vox Sang. 2021;116:1031–41. doi: 10.111/vox13103.
11. Lighthill MJ. On sound generated aerodynamically. I. General theory. Proc. R. Soc. Lond. A. 1952;211:564–87.
12. Chenyang W, Susann B, Ardeshir H. The attenuation of sound by turbulence in internal flows. J Acoust Soc Am. 2013;133:3764–76.
13. Twardowski Z, Haynie J, Moore H. Blood flow, negative pressure, and hemolysis during hemodialysis. Home Hemodial Int. 1999;3:45–50.
14. Ding J, Chen Z, Niu S, et al. Quantification of shear-induced platelet activation: High shear stresses for short exposure time. Artif Organs. 2015;39:576–83.